# AutoGrow: Automatic Layer Growing in Deep Convolutional Networks

Wei Wen
Duke University
Durham, North Carolina, United States
wei.wen@alumni.duke.edu

Yiran Chen
Duke University
Durham, North Carolina, United States
yiran.chen@duke.edu

# **ABSTRACT**

Depth is a key component of Deep Neural Networks (DNNs), however, designing depth is heuristic and requires many human efforts. We propose *AutoGrow* to automate depth discovery in DNNs: starting from a shallow seed architecture, *AutoGrow* grows new layers if the growth improves the accuracy; otherwise, stops growing and thus discovers the depth. We propose robust growing and stopping policies to generalize to different network architectures and datasets. Our experiments show that by applying the same policy to different network architectures, *AutoGrow* can always discover near-optimal depth on various datasets of MNIST, FashionMNIST, SVHN, CIFAR10, CIFAR100 and ImageNet. For example, in terms of accuracy-computation trade-off, *AutoGrow* discovers a better depth combination in *ResNets* than human experts. Our *AutoGrow* is efficient. It discovers depth within similar time of training a single DNN. Our code is available at https://github.com/wenwei202/autogrow.

# **CCS CONCEPTS**

• Computing methodologies → Neural networks; Computer vision; Discrete space search; Lifelong machine learning.

# **KEYWORDS**

automated machine learning; neural architecture search; neural networks; depth; growing

### **ACM Reference Format:**

Wei Wen, Feng Yan, Yiran Chen, and Hai Li. 2020. AutoGrow: Automatic Layer Growing in Deep Convolutional Networks. In Proceedings of the 26th ACM SIGKDD Conference on Knowledge Discovery and Data Mining (KDD '20), August 23–27, 2020, Virtual Event, USA. ACM, New York, NY, USA, 9 pages. https://doi.org/10.1145/3394486.3403126

Permission to make digital or hard copies of all or part of this work for personal or classroom use is granted without fee provided that copies are not made or distributed for profit or commercial advantage and that copies bear this notice and the full citation on the first page. Copyrights for components of this work owned by others than ACM must be honored. Abstracting with credit is permitted. To copy otherwise, or republish, to post on servers or to redistribute to lists, requires prior specific permission and/or a fee. Request permissions from permissions@acm.org.

KDD '20, August 23–27, 2020, Virtual Event, USA © 2020 Association for Computing Machinery. ACM ISBN 978-1-4503-7998-4/20/08...\$15.00 https://doi.org/10.1145/3394486.3403126

Feng Yan University of Nevada, Reno Reno, Nevada, United States fyan@unr.edu

# Hai Li

Duke University Durham, North Carolina, United States hai.li@duke.edu

### 1 INTRODUCTION

Layer depth is one of the decisive factors of the success of Deep Neural Networks (DNNs). For example, image classification accuracy keeps improving as the depth of network models grows [12, 15, 17, 32, 35]. Although shallow networks cannot ensure high accuracy, DNNs composed of too many layers may suffer from over-fitting and convergence difficulty in training. How to obtain the optimal depth for a DNN still remains mysterious. For instance, ResNet-152 [12] uses 3, 8, 36 and 3 residual blocks under output sizes of  $56 \times 56$ ,  $28 \times 28$ ,  $14 \times 14$  and  $7 \times 7$ , respectively, which don't show an obvious quantitative relation. In practice, people usually reply on some heuristic trials and tests to obtain the depth of a network: they first design a DNN with a specific depth and then train and evaluate the network on a given dataset; finally, they change the depth and repeat the procedure until the accuracy meets the requirement. Besides the high computational cost induced by the iteration process, such trial & test iterations must be repeated whenever dataset changes. In this paper, we propose AutoGrow that can automate depth discovery given a layer architecture. We will show that AutoGrow generalizes to different datasets and layer architectures.

There are some previous works which add or morph layers to increase the depth in DNNs. VggNet [32] and DropIn [33] added new layers into shallower DNNs; Network Morphism [5, 36, 37] morphed each layer to multiple layers to increase the depth meanwhile preserving the function of the shallower net. Table 1 summarizes differences in this work. Their goal was to overcome difficulty of training deeper DNNs or accelerate it. Our goal is to automatically find an optimal depth. Moreover, previous works applied layer growth by once or a few times at pre-defined locations to grow a pre-defined number of layers; in contrast, ours automatically learns the number of new layers and growth locations without limiting growing times. We will summarize more related works in Section 4.

Table 1: Comparison with previous works on layer growth.

	Previous works [5, 32, 33, 36, 37]	AutoGrow
Goal	Ease training	Depth automation
Growth times	Once or a few	Unlimited
Locations	Human defined	Learned
Layer #	Human defined	Learned

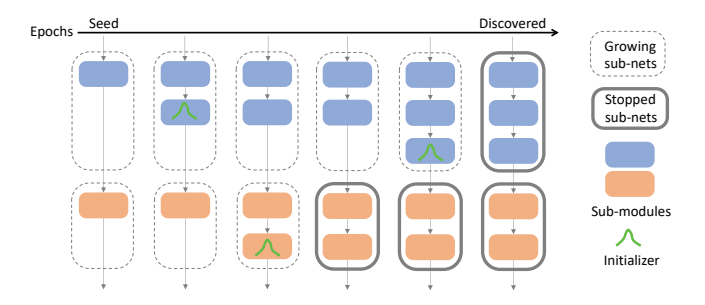


Figure 1: A simple example of AutoGrow.

Figure 1 illustrates an example of *AutoGrow*. It starts from the shallowest backbone network and gradually grows *sub-modules* (A *sub-module* can be one or more layers, *e.g.*, a residual block); the growth stops once a stopping policy is satisfied. We studied multiple initializers of new layers and multiple growing policies, and surprisingly find that: (1) a random initializer works equally or better than complicated Network Morphism; (2) it is more effective to grow *before* a shallow net converges. We hypothesize that this is because a converged shallow net is an inadequate initialization for training deeper net, while random initialization can help to escape from a bad starting point. Motivated by this, we intentionally avoid full convergence during the growing by using (1) random initialization of new layers, (2) a constant large learning rate, and (3) a short growing interval.

Our contributions are:

- We propose AutoGrow to automate DNN layer growing and depth discovery. AutoGrow is very robust. With the same hyper-parameters, it adapts network depth to various datasets including MNIST, FashionMNIST, SVHN, CIFAR10, CIFAR100 and ImageNet. Moreover, AutoGrow can also discover shallower DNNs when the dataset is a subset.
- AutoGrow demonstrates high efficiency and scales up to ImageNet, because the layer growing is as fast as training a single DNN. On ImageNet, it discovers a new ResNets with better trade-off between accuracy and computation complexity.
- We challenge the idea of Network Morphism, as random initialization works equally or better when growing layers.
- We find that it is beneficial to rapidly grow layers before a shallower net converge, contradicting previous intuition.

# 2 AUTOGROW – A DEPTH GROWING ALGORITHM

Figure 1 gives an overview of the proposed AutoGrow. In this paper, we use network, sub-networks, sub-modules and layers to describe the architecture hierarchy. A network is composed of a cascade of sub-networks. A sub-network is composed of sub-modules, which typical share the same output size. A sub-module (e.g. a residual block) is an elementary growing block composed of one or a few layers. In this section, we rigorously formulate a generic version of AutoGrow which will be materialized in subsections. A deep convolutional network  $g(X_0)$  is a cascade of sub-networks by composing functions as  $g(X_0) = l(f_{M-1}(f_{M-2}(\cdots f_1(f_0(X_0))\cdots)))$ , where  $X_0$  is an input image, M is the number of sub-networks,

# Algorithm 1 AutoGrow Algorithm.

#### Input:

A seed shallow network  $g(X_0)$  composed of M sub-networks  $\mathbb{F} = \{f_i(\cdot; \mathbb{W}_i) : i = 0 \dots M - 1\}$ , where each sub-network has only one sub-module (a dimension reduction sub-module); an epoch interval K to check growing and stopping policies; the number of fine-tuning epochs N after growing.

### Initialization:

```
A Circular Linked List of sub-networks under growing: subNetList = f_0(\cdot; \mathbb{W}_0) \to \cdots \to f_{M-1}(\cdot; \mathbb{W}_{M-1}); The current growing sub-network: growingSub = subNetList.head() = f_0(\cdot; \mathbb{W}_0); The last grown sub-network: grownSub = None;
```

#### **Process:**

```
# if there exist growing sub-network(s)
while subNetList.size()>0 do
  train(g(X_0), K) # train the whole network g(X_0) for K epochs
  if meetStoppingPolicy() then
     # remove a sub-network from the growing list
     subNetList.delete(grownSub);
  end if
  if meetGrowingPolicy() and subNetList.size()>0 then
     # the current growing sub-network growingSub
     f_i\left(\cdot;\mathbb{W}_i\right)
     \mathbb{W}_i = \mathbb{W}_i \cup \mathcal{W} # stack a sub-module on top of f_i(\cdot; \mathbb{W}_i)
     initializer (W); # initialize the new sub-module W
     grownSub = growingSub;
     growingSub = subNetList.next(growingSub);
  end if
end while
```

# Output:

A trained neural network  $q(X_0)$  with learned depth.

Fine-tune the discovered network  $q(X_0)$  for N epochs;

 $l(\cdot)$  is a loss function, and  $X_{i+1} = f_i \ (X_i)$  is a sub-network that operates on an input image or a feature tensor  $X_i \in \mathbb{R}^{c_i \times h_i \times w_i}$ . Here,  $c_i$  is the number of channels, and  $h_i$  and  $w_i$  are spatial dimensions.  $f_i \ (X_i)$  is a simplified notation of  $f_i \ (X_i; \mathbb{W}_i)$ , where  $\mathbb{W}_i$  is a set of sub-modules parameters within the i-th sub-network. Thus  $\mathbb{W} = \{\mathbb{W}_i : i = 0 \dots M-1\}$  denotes the whole set of parameters in the DNN. To facilitate growing, the following properties are supported within a sub-network: (1) the first sub-module usually reduces the size of input feature maps, e.g., using pooling or convolution with a stride; and (2) all sub-modules in a sub-network maintain the same output size. As such, our framework can support popular networks, including VggNet-like plain networks [32], GoogLeNet [35], ResNets [12] and DenseNets [15]. In this paper, we select ResNets and VggNet-like nets as representatives of DNNs with and without shortcuts, respectively.

With above notations, Algorithm 1 rigorously describes the *AutoGrow* algorithm. In brief, *AutoGrow* starts with the shallowest net

where every sub-network has only one sub-module for spatial dimension reduction. *AutoGrow* loops over all growing sub-networks in order. For each sub-network, *AutoGrow* stacks a new sub-module. When the new sub-module does not improve the accuracy, the growth in corresponding sub-network will be permanently stopped. The details of our method will be materialized in the following subsections.

# 2.1 Seed Shallow Networks and Sub-modules

In this paper, in all datasets except ImageNet, we explore growing depth for four types of DNNs:

- Basic3ResNet: the same ResNet used for CIFAR10 in [12], which has 3 residual sub-networks with output spatial sizes of 32 × 32, 16 × 16 and 8 × 8, respectively;
- Basic4ResNet: a variant of *ResNet* used for ImageNet in [12] built by basic residual blocks (each of which contains two convolutions and one shortcut). There are 4 *sub-networks* with output spatial sizes of 32 × 32, 16 × 16, 8 × 8 and 4 × 4, respectively;
- Plain3Net: a VggNet-like plain net by removing shortcuts in Basic3ResNet;
- Plain4Net: a VggNet-like plain net by removing shortcuts in Basic4ResNet.

In *AutoGrow*, the architectures of seed shallow networks and sub-modules are pre-defined. In plain DNNs, a *sub-module* is a stack of convolution, Batch Normalization and ReLU; in residual DNNs, a *sub-module* is a residual block. In *AutoGrow*, a *sub-network* is a stack of all sub-modules with the same output spatial size. Unlike [12] which manually designed the depth, *AutoGrow* starts from a seed architecture in which each sub-network has only one sub-module and automatically learns the number of sub-modules.

On ImageNet, we apply the same backbones in [12] as the seed architectures. A seed architecture has only one sub-module under each output spatial size. For a *ResNet* using basic residual blocks or bottleneck residual blocks [12], we respectively name it as Basic4ResNet or Bottleneck4ResNet. Plain4Net is also obtained by removing shortcuts in Basic4ResNet.

### 2.2 Sub-module Initializers

Here we explain how to initialize a new sub-module  $\mathcal{W}$  mentioned in Algorithm 1 (initializer( $\mathcal{W}$ )). Network Morphism changes DNN architecture meanwhile preserving the loss function via special initialization of new layers, that is,

$$g(X_0; \mathbb{W}) = g(X_0; \mathbb{W} \cup \mathcal{W}) \ \forall X_0. \tag{1}$$

A residual sub-module shows a nice property: when stacking a residual block and initializing the last Batch Normalization layer as zeros, the function of the shallower net is preserved but the DNN is morphed to a deeper net. Thus, Network Morphism can be easily implemented by this zero initialization (ZeroInit).

In this work, all layers in  $\mathcal{W}$  are initialized using default randomization, except for a special treatment of the last Batch Normalization layer in a *residual* sub-module. Besides ZeroInit, we propose a new AdamInit for Network Morphism. In AdamInit, we freeze all parameters except the last Batch Normalization layer in  $\mathcal{W}$ , and then use Adam optimizer [16] to optimize the last Bath

Normalization for maximum 10 epochs till the training accuracy of the deeper net is as good as the shallower one. After AdamInit, all parameters are jointly optimized. We view AdamInit as a Network Morphism because the training loss is similar after AdamInit. We empirically find that AdamInit can usually find a solution in less than 3 epochs. We also study random initialization of the last Batch Normalization layer using uniform (UniInit) or Gaussian (GauInit) noises with a standard deviation 1.0. We will show that GauInit obtains the best result, challenging the idea of Network Morphism [5, 36, 37].

# 2.3 Growing and Stopping Policies

In Algorithm 1, a growing policy refers to meetGrowingPolicy(), which returns true when the network should grow a sub-module. Two growing policies are studied here:

- (1) Convergent Growth: meetGrowingPolicy() returns true when the improvement of validation accuracy is less than  $\tau$  in the last K epochs. That is, in Convergent Growth, AutoGrow only grows when current network has converged. This is a similar growing criterion adopted in previous works [3, 4, 9].
- (2) Periodic Growth: meetGrowingPolicy() always returns true, that is, the network always grows every K epochs. Therefore, K is also the growing period. In the best practice of AutoGrow, K is small (e.g. K = 3) such that it grows before current network converges.

Our experiments will show that Periodic Growth outperforms Convergent Growth. We hypothesize that a fully converged shallower net is an inadequate initialization to train a deeper net. We will perform experiments to test this hypothesis and visualize optimization trajectory to illustrate it.

A stopping policy denotes meetStoppingPolicy() in Algorithm 1. When Convergent Growth is adopted, meetStoppingPolicy() returns true if a recent growth does not improve validation accuracy more than  $\tau$  within K epochs. We use a similar stopping policy for Periodic Growth; however, as it can grow rapidly with a small period K (e.g. K=3) before it converges, we use a larger window size J for stop. Specifically, when Periodic Growth is adopted, meetStoppingPolicy() returns true when the validation accuracy improves less than  $\tau$  in the last J epochs, where  $J\gg K$ .

Hyper-parameters  $\tau$ , J and K control the operation of AutoGrow and can be easily setup and generalize well.  $\tau$  denotes the significance of accuracy improvement for classification. We simply set  $\tau=0.05\%$  in all experiments. J represents how many epochs to wait for an accuracy improvement before stopping the growth of a sub-network. It is more meaningful to consider stopping when the new net is trained to some extent. As such, we set J to the number of epochs T under the largest learning rate when training a baseline. K means how frequently AutoGrow checks the polices. In Convergent Growth, we simply set K=T, which is long enough to ensure convergence. In Periodic Growth, K is set to a small fraction of T to enable fast growth before convergence; more importantly, K=3 is very robust to all networks and datasets. Therefore, all those hyper-parameters are very robust and strongly correlated to design considerations.

Table 2: Network Morphism tested on CIFAR10.

net backbone	shallower	deeper	initializer	accu %	$\Delta^*$
Basic3ResNet	3-3-3	5-5-5	ZeroInit AdamInit	92.71 92.82	-0.77 -0.66
Basic3ResNet	5-5-5	9-9-9	ZeroInit AdamInit	93.64 93.53	-0.27 -0.38
Basic4ResNet	1-1-1-1	2-2-2-2	ZeroInit AdamInit	94.96 95.17	-0.37 -0.16

<sup>\*</sup>  $\Delta$  = (accuracy of Network Morphism) – (accuracy of training from scratch)

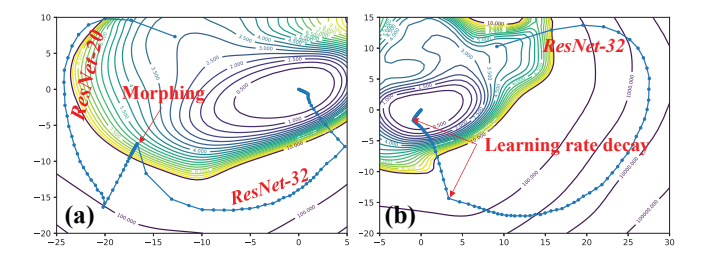


Figure 2: An optimization trajectory comparison between (a) Network Morphism and (b) training from scratch.

## 3 EXPERIMENTS

In this paper, we use Basic3ResNet-2-3-2, for instance, to denote a model architecture which contains 2, 3 and 2 sub-modules in the first, second and third sub-networks, respectively. Sometimes we simplify it as 2-3-2 for convenience. *AutoGrow* always starts from the shallowest depth of 1-1-1 and uses the maximum validation accuracy as the metric to guide growing and stopping. All DNN baselines are trained by SGD with momentum 0.9 using staircase learning rate. The initial learning rate is 0.1 in *ResNets* and 0.01 in plain networks. On ImageNet, baselines are trained using batch size 256 for 90 epochs, within which learning rate is decayed by 0.1× at epoch 30 and 60. In all other smaller datasets, baselines are trained using batch size 128 for 200 epochs and learning rate is decayed by 0.1× at epoch 100 and 150.

Our early experiments followed prior wisdom by growing layers with Network Morphism [3–5, 9, 36, 37], *i.e.*, *AutoGrow* with ZeroInit (or AdamInit) and Convergent Growth policy; however, it stopped early with very shallow DNNs, failing to find optimal depth. We hypothesize that a converged shallow net with Network Morphism gives a bad initialization to train a deeper neural network. Section 3.1 experimentally test that the hypothesis is valid. To tackle this issue, we intentionally avoid convergence during growing by three simple solutions, which are evaluated in Section 3.2. Finally, Section 3.3 and Section 3.4 include extensive experiments to show the effectiveness of our final *AutoGrow*.

# 3.1 Suboptimum of Network Morphism and Convergent Growth

In this section, we study Network Morphism itself and its integration into our *AutoGrow* under Convergent Growth. When studying Network Morphism, we take the following steps: 1) train a shallower *ResNet* to converge, 2) stack residual blocks on top of each

sub-network to morph to a deeper net, 3) use ZeroInit or AdamInit to initialize new layers, and 4) train the deeper net in a standard way. We compare the accuracy difference (" $\Delta$ ") between Network Morphism and training the deeper net from scratch. Table 2 summaries our results. Network Morphism has a lower accuracy (negative " $\Delta$ ") in all the cases, which validates our hypothesis that a converged shallow network with Network Morphism gives a bad initialization to train a deeper net.

We visualize the optimization trajectories to illustrate the hypothesis. We hypothesize that a converged shallower net may not be an adequate initialization. Figure 2 visualizes and compares the optimization trajectories of Network Morphism and the training from scratch. In this figure, the shallower net is Basic3ResNet-3-3-3 (ResNet-20) and the deeper one is Basic3ResNet-5-5-5 (ResNet-32) in Table 2. The initializer is ZeroInit. The visualization method is extended from [20]. Points on the trajectory are evenly sampled every a few epochs. To maximize the variance of trajectory, we use PCA to project from a high dimensional space to a 2D space and use the first two Principle Components (PC) to form the axes in Figure 2. The contours of training loss function and the trajectory are visualized around the final minimum of the deeper net. When projecting a shallower net to a deeper net space, zeros are padded for the parameters not existing in the deeper net. We must note that the loss increase along the trajectory does not truly represent the situation in high dimensional space, as the trajectory is just a projection. It is possible that the loss remains decreasing in the high dimension while it appears in an opposite way in the 2D space. The sharp detour at "Morphing" in Figure 2(a) may indicate that the shallower net plausibly converges to a point that the deeper net struggles to escape. In contrast, Figure 2(b) shows that the trajectory of the direct optimization in the deeper space smoothly converges to a better minimum.

To further validate our hypothesis, we integrate Network Morphism as the initializer in AutoGrow with Convergent Growth policy. We refer to this version of *AutoGrow* as *c-AutoGrow* with "*c-*" denoting "Convergent." More specific, we take ZeroInit or AdamInit as sub-module initializer and "Convergent Growth" policy in Algorithm 1. To recap, in this setting, AutoGrow trains a shallower net till it converges, then grows a sub-module which is initialized by Network Morphism, and repeats the same process till there is no further accuracy improvement. In every interval of K training epochs (train( $q(X_0), K$ ) in Algorithm 1), "staircase" learning rate is used. The learning rate is reset to 0.1 at the first epoch, and decayed by 0.1× at epoch  $\frac{K}{2}$  and  $\frac{3K}{4}$ . The results are shown in Table 3 by "staircase" rows, which illustrate that c-AutoGrow can grow a DNN multiple times and finally find a depth. However, there are two problems: 1) the final accuracy is lower than training the found net from scratch, as indicated by " $\Delta$ ", validating our hypothesis; 2) the depth learning stops too early with a relatively shallower net, while a deeper net beyond the found depth can achieve a higher accuracy as we will show in Table 4. These problems provide a circumstantial evidence of the hypothesis that a converged shallow net with Network Morphism gives a bad initialization. Thus, AutoGrow cannot receive signals to continue growing after a limited number of growths.

Table 3: Ab	lation s	tudy of	c-AutoGrow.
-------------	----------	---------	-------------

dataset	learning rate	initializer	found net <sup>†</sup>	accu %	$\Delta^*$	dataset	learning rate	initializer	found net <sup>†</sup>	accu %	$\Delta^*$
		7	2.2.6	01.77	1.06			7	4 2 4	70.04	0.75
	<u>staircase</u>	ZeroInit	2-3-6	91.77	-1.06		<u>staircase</u>	ZeroInit	4-3-4	70.04	-0.65
	<u>staircase</u>	AdamInit	3-4-3	92.21	-0.59		<u>staircase</u>	AdamInit	3-3-3	69.85	-0.65
CIFAR10	constant	ZeroInit	2-2-4	92.23	0.16	CIFAR100	constant	ZeroInit	3-2-4	70.22	0.35
	constant	AdamInit	3-4-4	92.60	-0.41		constant	AdamInit	3-3-3	70.00	-0.50
	constant	UniInit	3-4-4	92.93	-0.08		constant	UniInit	4-4-3	70.39	0.36
	constant	GauInit	2-4-3	93.12	0.55		constant	GauInit	3-4-3	70.66	0.91
-1-											

<sup>†</sup>Basic3ResNet

<sup>\*</sup>  $\Delta = (accuracy of c-AutoGrow) - (accuracy of training from scratch)$ 

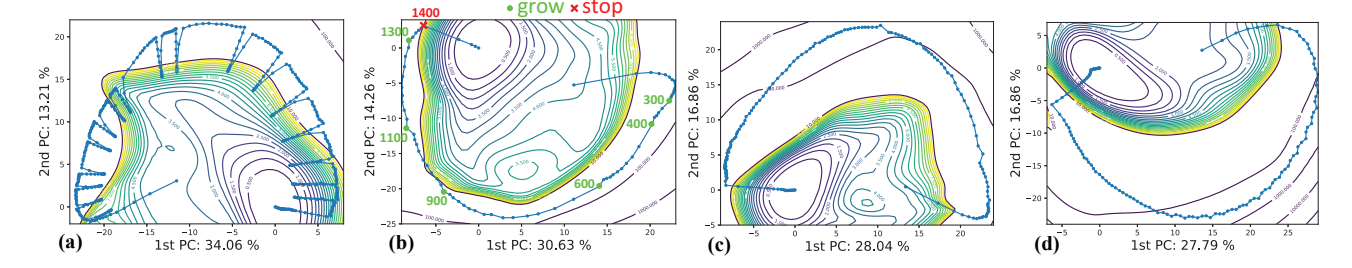


Figure 3: Optimization trajectory of AutoGrow, tested by Basic3ResNet on CIFAR10. (a) c-AutoGrow with staircase learning rate and ZeroInit during growing; (b) c-AutoGrow with constant learning rate and GauInit during growing; (c) p-AutoGrow with K = 50; and (d) p-AutoGrow with K = 3. For better illustration, the dots on the trajectory are plotted every 4, 20, 5 and 3 epochs in (a-d), respectively.

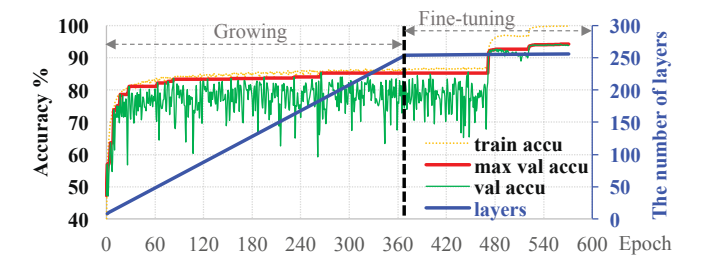


Figure 4: p-AutoGrow on CIFAR10 (K = 3). The seed net is Basic3ResNet-1-1-1.

Figure 3(a) visualizes the trajectory of *c-AutoGrow* corresponding to row "2–3–6" in Table 3. Along the trajectory, there are many trials to detour and escape an initialization from a shallower net.

# 3.2 Ablation Study for *AutoGrow* Design

Based on the findings in Section 3.1, we propose three simple but effective solutions to further enhance *AutoGrow* and refer it as *p-AutoGrow*, with "*p-*" denoting "Periodic":

 Use a *large constant* learning rate for growing, *i.e.*, 0.1 for residual networks and 0.01 for plain networks. Stochastic gradient descent with a large learning rate intrinsically introduces noises, which help to avoid a full convergence into a bad initialization from a shallower net. Note that staircase learning rate is still used for fine-tuning after discovering the final DNN;

- Use random initialization (UniInit or GauInit) as noises to escape from an inadequate initialization;
- Grow rapidly *before* a shallower net converges by taking Periodic Growth with a small *K*.

p-AutoGrow is our final AutoGrow. In the rest part of this section, we perform ablation study to prove that the three solutions are effective. We start from c-AutoGrow, and incrementally add above solutions one by one and eventually obtain p-AutoGrow. In Table 3, first, we replace the staircase learning rate with a constant large learning rate, the accuracy of AutoGrow improves and therefore "Δ" improves; second, we further replace Network Morphism (ZeroInit or AdamInit) with a random initializer (UniInit or GauInit) and result in a bigger gain. Overall, combining a constant learning rate with GauInit performs the best. Thus, constant learning rate and GauInit are adopted in the remaining experiments, unless we explicitly specify them. Figure 3(b) visualizes the trajectory corresponding to row "2-4-3" in Table 3, which is much smoother compared to Figure 3(a), implying the advantages of constant large learning rate and GauInit.

Note that, in this paper, we are more interested in automating depth discovery to find a final DNN ("found net") with a high accuracy ("accu"). Ideally, the "found net" has a minimum depth, a larger depth than which cannot further improve "accu". We will show in Figure 5 that AutoGrow discovers a depth approximately satisfying this property. The " $\Delta$ " is a metric to indicate how well shallower nets initialize deeper nets; a negative " $\Delta$ " indicates that weight initialization from a shallower net hurts training of a deeper

Table 5: *p-AutoGrow* with different growing interval *K*.

50     6-5-3     92.95     50     8-5-7       20     7-7-7     93.26     20     8-11-10       10     19-19-19     93.46     10     18-18-18       5     23-22-22     93.98     5     23-23-23		CIFAR10			CIFAR100			
20 7-7-7 93.26 20 8-11-10 10 19-19-19 93.46 10 18-18-18 15 23-22-22 93.98 5 23-23-23	K	found net $^\dagger$	accu %	K	found net $^\dagger$	accu %		
10 19-19-19 93.46 10 18-18-18 15 23-22-22 93.98 5 23-23-23	50	6-5-3	92.95	50	8-5-7	72.07		
5 23-22-22 93.98 5 23-23-23	20	7-7-7	93.26	20	8-11-10	72.93		
	10	19-19-19	93.46	10	18-18-18	73.64		
3 42-42-42 94.27 3 54-53-53 5	5	23-22-22	93.98	5	23-23-23	73.70		
3 TE TE TE 75.27 3 37 33 33	3	42-42-42	94.27	3	54-53-53	74.72		
1 77-76-76 94.30 1 68-68-68 1 The state of t	1	77-76-76	94.30	_ 1	68-68-68	74.51		

†Basic3ResNet

†Basic3ResNet

Table 6: p-AutoGrow under initializers with K = 3.

	CIFAR10		•		CIFAR100	
initializer	found net <sup>†</sup>	accu		initializer	found $\mathrm{net}^\dagger$	accu
ZeroInit	31-30-30	93.57		ZeroInit	26-25-25	73.45
AdamInit	37-37-36	93.79		AdamInit	27-27-27	73.92
UniInit	28-28-28	93.82		UniInit	41-41-41	74.31
GauInit	42-42-42	94.27		GauInit	54-53-53	74.72

†Basic3ResNet

†Basic3ResNet

net; while a positive "\Delta" indicates *AutoGrow* helps training a deeper net, which is a byproduct of this work.

Finally, we apply the last solution – Periodic Growth, and obtain our final p-AutoGrow. Our ablation study results for p-AutoGrow are summarized in Table 5. Table 5 analyzes the impact of the growing period K. In general, K is a hyper-parameter to trade off speed and accuracy: a smaller K takes a longer learning time but discovers a deeper net, vice versa. Our results validate the preference of a faster growth (i.e. a smaller K). On CIFAR10/CIFAR100, the accuracy reaches plateau/peak at K=3; further reducing K produces a deeper net while the accuracy gain is marginal/impossible. In the following, we simply select K=3 for robustness test. More importantly, our quantitative results in Table 5 show that p-AutoGrow finds much deeper nets, overcoming the very-early stop issue in c-AutoGrow in Table 3. That is, Periodic Growth proposed in this work is much more effective than Convergent Growth utilized in previous work.

Figure 3(c)(d) visualize the trajectories of p-AutoGrow with K = 50 and 3. The 2D projection gives limited information to reveal the

Table 7: p-AutoGrow with different seed architecture.

dataset	seed net $^\dagger$	found $\mathrm{net}^\dagger$	accuracy %
CIFAR10	1-1-1	42-42-42	94.27
CIFARIO	5-5-5	46-46-46	94.16
CIFAR10	1-1-1-1	22-22-22	95.49
	5-5-5-5	23-22-22-22	95.62

<sup>†</sup>Basic3ResNet or Basic4ResNet.

advantages of *p-AutoGrow* comparing to *c-AutoGrow* in Figure 3(b), although the trajectory of our final *p-AutoGrow* in Figure 3(d) is plausibly more similar to the one of training from scratch in Figure 2(b).

For sanity check, we perform the ablation study of initializers for *p-AutoGrow*. The results are in Table 6, which further validates our wisdom on selecting GauInit. The motivation of Network Morphism in previous work was to start a deeper net from a loss function that has been well optimized by a shallower net, so as not to restart the deeper net training from scratch [3–5, 9, 36, 37]. In all our experiments, we find that simple random initialization can achieve the same goal. Figure 4 plots the convergence curves and learning process for "42–42–42" in Table 5. Even with GauInit, the loss and accuracy rapidly recover and no restart is observed. The convergence pattern in the "Growing" stage is similar to the "Fine-tuning" stage under the same learning rate (the initial learning rate 0.1). Similar results on ImageNet will be shown in Figure 8. Our results challenge the necessity of Network Morphism when growing neural networks.

At last, we perform the ablation study on the initial depth of the seed network. Table 7 demonstrates that a shallowest DNN works as well as a deeper seed. This implies that *AutoGrow* can appropriately stop regardless of the depth of the seed network. As the focus of this work is on depth automation, we prefer starting with the shallowest seed to avoid a manual search of a seed depth.

# 3.3 Adaptability of AutoGrow

To verify the adaptability of AutoGrow, we use an identical configuration (p-AutoGrow with K=3) and test over 5 datasets and 4 seed architectures. Table 4 includes the results of all 20 combinations.

Table 4: The adaptability of AutoGrow to datasets

net	dataset	found net	accu %	$\Delta^*$
	CIFAR10	42-42-42	94.27	-0.03
	CIFAR100	54-53-53	74.72	-0.95
Basic3ResNet	SVHN	34-34-34	97.22	0.04
	FashionMNIST	30-29-29	94.57	-0.06
	MNIST	33-33-33	99.64	-0.03
	CIFAR10	22-22-22	95.49	-0.10
	CIFAR100	17-51-16-16	79.47	1.22
Basic4ResNet	SVHN	20-20-19-19	97.32	-0.08
	FashionMNIST	27-27-27-26	94.62	-0.17
	MNIST	11-10-10-10	99.66	0.01

<sup>\*</sup>  $\Delta$  = (accuracy of *AutoGrow*) – (accuracy of training from scratch)

dataset found net accu % CIFAR10 23-22-22 90.82 6.49 CIFAR100 28-28-27 66.34 31.53 Plain3Net **SVHN** 36-35-35 96.79 77.20 FashionMNIST 17-17-17 94.49 0.56 20-20-20 MNIST 99.66 CIFAR10 17-17-17-17 94.20 5.72 CIFAR100 16-15-15-15 73.91 29.34 Plain4Net **SVHN** 12-12-12-11 97.08 0.32 FashionMNIST 13-13-13-13 0.72 94.47 **MNIST** 13-12-12-12 99.57 0.03

Figure 5 compares *AutoGrow* with manual search which is obtained by training many DNNs with different depths from scratch. The results lead to the following conclusions and contributions:

- (1) In Table 4, AutoGrow discovers layer depth across all scenarios without any tuning, achieving the main goal of this work. Manual design needs  $m \cdot n \cdot k$  trials, where m and n are respectively the numbers of datasets and sub-module categories, and k is the number of trials per dataset per sub-module category;
- (2) For ResNets, a discovered depth ("●" in Figure 5) falls at the location where accuracy saturates. This means AutoGrow discovers a near-optimal depth: a shallower depth will lose accuracy while a deeper one gains little. The final accuracy of AutoGrow is as good as training the discovered net from scratch as indicated by " $\Delta$ " in Table 4, indicating that initialization from shallower nets does not hurt training of deeper nets. As a byproduct, in plain networks, there are large positive "Δ"s in Table 4. It implies that baselines fail to train very deep plain networks even using Batch Normalization, but AutoGrow enables the training of these networks; Table 9 shows the accuracy improvement of plain networks by tuning *K*, approaching the accuracy of *ResNets* with the same depth. Figure 6 visualizes loss surfaces around minima by AutoGrow and baseline. Intuitively, AutoGrow finds wider or deeper minima with less chaotic landscapes.
- (3) For robustness and generalization study purpose, we stick to K = 3 in our experiments, however, we can tune K to trade off accuracy and model size. As shown in Figure 5, AutoGrow discovers smaller DNNs when increasing K from 3 ("●") to 50 ("○"). Interestingly, the accuracy of plain networks even increases at K = 50. This implies the possibility of discovering a better accuracy-depth trade-off by tuning K, although we stick to K = 3 for generalizability study and it generalizes well.
- (4) In Table 4, *AutoGrow* discovers different depths under different sub-modules. The final accuracy is limited by the sub-module design, not by our *AutoGrow*. Given a sub-module architecture, our *AutoGrow* can always find a near-optimal depth.

Finally, our supposition is that: when the size of dataset is smaller, the optimal depth should be smaller. Under this supposition, we test the effectiveness of AutoGrow by sampling a subset of dataset and verify if AutoGrow can discover a shallower depth. Table 8 summarizes the results. In each set of experiments, dataset is randomly down-sampled to 100%, 75%, 50% and 25%. For a fair comparison, K is divided by the percentage of dataset such that the number of mini-batches between growths remains the same. As expected, our

experiments show that *AutoGrow* adapts to shallower networks when the datasets are smaller.

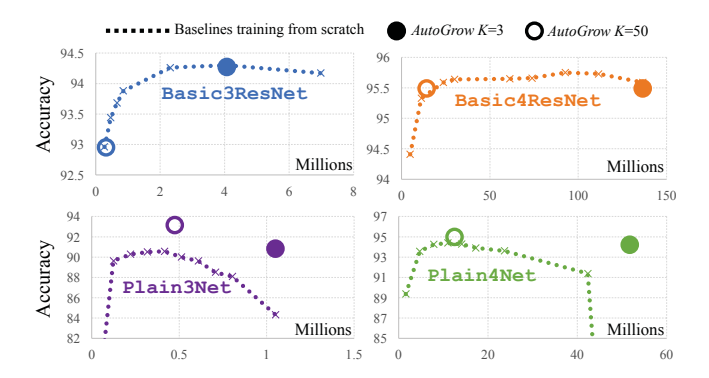


Figure 5: AutoGrow vs manual search obtained by training many baselines from scratch. x - axis is the number of parameters. Dataset is CIFAR10.

Table 9: AutoGrow improves accuracy of plain nets.

dataset	net	layer #	method	accu %
	Plain4Net-6-6-6-6	26	baseline	93.90
CIFAR10	Plain4Net-6-6-6-6	26	$AutoGrow \\ K = 30$	95.17
	Basic4ResNet-3-3-3-3	26	baseline	95.33
	Plain3Net-11-11-10	34	baseline	90.45
CIFAR10	Plain3Net-11-11-10	34	$AutoGrow \\ K = 50$	93.13
	Basic3ResNet-6-6-5	36	baseline	93.60

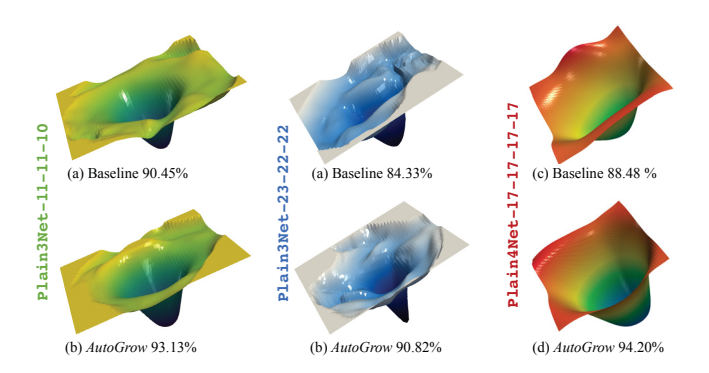


Figure 6: Loss surfaces around minima found by baselines and *AutoGrow*. Dataset is CIFAR10.

Table 8: The adaptability of AutoGrow to dataset sizes

Basic3ResNet on CIFAR10				Basic4ResNet on CIFAR100			
dataset size	found net	accu %		dataset size	found net	accu %	d
100%	42-42-42	94.27		100%	17-51-16-16	79.47	
75%	32-31-31	93.54		75%	17-17-16-16	77.26	
50%	17-17-17	91.34		50%	12-12-12-11	72.91	
25%	21-12-7	88.18		25%	6-6-6-6	62.53	

Plain3	P.		
dataset size	dataset size found net accu %		dataset siz
100%	20-20-20	99.66	100%
75%	12-12-12	99.54	75%
50%	12-11-11	99.46	50%
25%	10-9-9	99 33	25%

Plain4Net on SVHN								
dataset size	found net	accu %						
100%	12-12-12-11	97.08						
75%	9-9-9-9	96.71						
50%	8-8-8-8	96.37						
25%	5-5-5-5	95.68						

Table 10: Scaling up to ImageNet

net	K	found net	Top-1	Top-5	<sup>†</sup> Δ Top-1
Basic4ResNet	2	12-12-11-11	76.28	92.79	0.43
	5	9-3-6-4	74.75	91.97	0.72
Bottleneck4ResNet	2	6-6-6-17	77.99	93.91	0.83
	5	6-7-3-9	77.33	93.65	0.83
Plain4Net	2 5	6-6-6-6 5-5-5-4	71.22 70.54	90.08 89.76	0.70 0.93

 $<sup>^{\</sup>dagger}$   $\Delta$  = (Top-1 of *AutoGrow*) – (Top-1 of training from scratch)

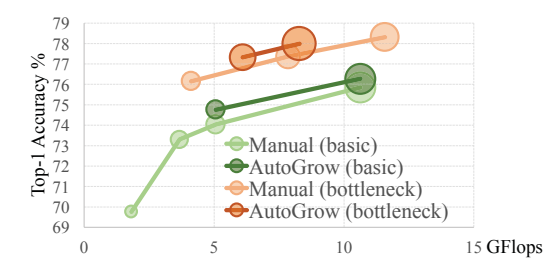


Figure 7: AutoGrow vs. manual design [12] on ImageNet. Marker area is proportional to model size determined by depth. "basic" ("bottleneck") refers to ResNets with basic (bottleneck) residual blocks.

# 3.4 Scaling to ImageNet and Efficiency

In ImageNet, K=3 should generalize well, but we explore Auto-Grow with K=2 and K=5 to obtain an accuracy-depth trade-off line for comparison with human experts. The larger K=5 enables AutoGrow to obtain a smaller DNN to trade-off accuracy and model size (computation) and the smaller K=2 achieves higher accuracy. The results are shown in Table 10, which proves that AutoGrow automatically finds a good depth without any tuning. As a byproduct, the accuracy is even higher than training the found net from scratch, indicating that the Periodic Growth in AutoGrow helps training deeper nets. The comparison of AutoGrow and manual depth design [12] is in Figure 7, which shows that AutoGrow achieves better trade-off between accuracy and computation (measured by floating point operations).

Table 11 summarizes the breakdown of wall-clock time in AutoGrow. The growing/searching time is as efficient as (often more efficient than) fine-tuning the single discovered DNN. The scalability of AutoGrow comes from its intrinsic features that (1) it grows quickly with a short period K and stops immediately if no improvement is sensed; and (2) the network is small at the beginning of growing. Figure 8 plots the growing and converging curves for two DNNs in Table 11. Even with random initialization in new layers, the accuracy converges stably.

### 4 RELATED WORK

Neural Architecture Search (NAS) [42] and neural evolution [1, 22, 26, 30, 34] can search network architectures from a gigantic search space. In NAS, the depth of DNNs in the search space is fixed, while *AutoGrow* learns the depth. Some NAS methods [2, 6, 23] can find DNNs with different depths, however, the maximum depth is pre-defined and shallower depths are obtained by padding zero

Table 11: The efficiency of AutoGrow

net	GPUs	growing	fine-tuning
Basic4ResNet-12-12-11-11	4 GTX 1080 Ti	56.7 hours	157.9 hours
Basic4ResNet-9-3-6-4	4 GTX 1080	47.9 hours	65.8 hours
Bottleneck4ResNet-6-6-6-17	4 TITAN V	45.3 hours	114.0 hours
Bottleneck4ResNet-6-7-3-9	4 TITAN V	61.6 hours	78.6 hours
Plain4Net-6-6-6-6	4 GTX 1080 Ti	11.7 hours	29.7 hours
Plain4Net-5-5-5-4	4 GTX 1080 Ti	25.6 hours	25.3 hours

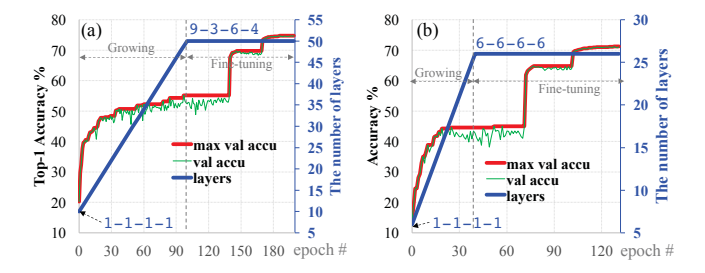


Figure 8: The convergence curves and growing process on ImageNet for (a) Basic4ResNet-9-3-6-4 and (b) Plain4Net-6-6-6-6 in Table 11.

operations or selecting shallower branches, while our *AutoGrow* learns the depth in an open domain to find a minimum depth, beyond which no accuracy improvement can be obtained. Moreover, NAS is very computation and memory intensive. To accelerate NAS, one-shot models [2, 28, 31], DARTS [23] and NAS with Transferable Cell [21, 43] were proposed. The search time reduces dramatically but is still long from practical perspective. It is still very challenging to deploy these methods to larger datasets such as ImageNet. In contrast, our *AutoGrow* can scale up to ImageNet thanks to its short depth learning time, which is as efficient as training a single DNN.

In addition to architecture search which requires to train lots of DNNs from scratch, there are also many studies on learning neural structures within a single training. Structure pruning and growing were proposed for different goals, such as efficient inference [7, 8, 11, 13, 14, 18, 19, 24, 25, 27, 38–40], lifelong learning [41] and model adaptation [10, 29]. However, those works fixed the network depth and limited structure learning within the existing layers. Optimization over a DNN with fixed depth is easier as the skeleton architecture is known. *AutoGrow* performs in a scenario where the DNN depth is unknown hence we must seek for the optimal depth.

# 5 CONCLUSION

In this paper, we propose a simple but effective layer growing algorithm (*AutoGrow*) to automate the depth design of deep neural networks. We empirically show that *AutoGrow* can adapt to different datasets for different layer architectures without tuning hyper-parameters. *AutoGrow* can significantly reduce human effort on searching layer depth. We surprisingly find that a rapid growing (under a large constant learning rate with random initialization of new layers) outperforms more intuitively-correct growing method, such as Network Morphism growing after a shallower net converged. We believe our initiative results can inspire future research on structure growth of neural networks and related theory.

Acknowledgments. This work was supported in part by NSF CCF-1725456, NSF 1937435, NSF 1822085, NSF CCF-1756013, NSF IIS-1838024 and DOE DE-SC0018064. Any opinions, findings, conclusions or recommendations expressed in this material are those of the authors and do not necessarily reflect the views of NSF, DOE or its contractors. We also thank Dr. Yandan Wang (yandonw@unr.edu) at University of Nevada Reno for valuable feedback on this work.

### **REFERENCES**

- Peter J Angeline, Gregory M Saunders, and Jordan B Pollack. 1994. An evolutionary algorithm that constructs recurrent neural networks. *IEEE transactions on Neural Networks* 5, 1 (1994), 54–65.
- [2] Gabriel Bender, Pieter-Jan Kindermans, Barret Zoph, Vijay Vasudevan, and Quoc Le. 2018. Understanding and simplifying one-shot architecture search. In International Conference on Machine Learning. 549–558.
- [3] Han Cai, Tianyao Chen, Weinan Zhang, Yong Yu, and Jun Wang. 2018. Efficient architecture search by network transformation. In Thirty-Second AAAI Conference on Artificial Intelligence.
- [4] Han Cai, Jiacheng Yang, Weinan Zhang, Song Han, and Yong Yu. 2018. Pathlevel network transformation for efficient architecture search. arXiv preprint arXiv:1806.02639 (2018).
- [5] Tianqi Chen, Ian Goodfellow, and Jonathon Shlens. 2015. Net2net: Accelerating learning via knowledge transfer. arXiv preprint arXiv:1511.05641 (2015).
- [6] Corinna Cortes, Xavier Gonzalvo, Vitaly Kuznetsov, Mehryar Mohri, and Scott Yang. 2017. Adanet: Adaptive structural learning of artificial neural networks. In Proceedings of the 34th International Conference on Machine Learning-Volume 70. IMLR. org, 874–883.
- [7] Xiaoliang Dai, Hongxu Yin, and Niraj K Jha. 2017. NeST: A neural network synthesis tool based on a grow-and-prune paradigm. arXiv:1711.02017 (2017).
- [8] Xiaocong Du, Zheng Li, and Yu Cao. 2019. CGaP: Continuous Growth and Pruning for Efficient Deep Learning. arXiv preprint arXiv:1905.11533 (2019).
- [9] Thomas Elsken, Jan-Hendrik Metzen, and Frank Hutter. 2017. Simple and Efficient Architecture Search for CNNs. In Workshop on Meta-Learning (MetaLearn 2017) at NIPS.
- [10] Jiashi Feng and Trevor Darrell. 2015. Learning the structure of deep convolutional networks. In Proceedings of the IEEE international conference on computer vision. 2749–2757.
- [11] Ariel Gordon, Elad Eban, Ofir Nachum, Bo Chen, Hao Wu, Tien-Ju Yang, and Edward Choi. 2018. Morphnet: Fast & simple resource-constrained structure learning of deep networks. In Proceedings of the IEEE Conference on Computer Vision and Pattern Recognition. 1586–1595.
- [12] Kaiming He, Xiangyu Zhang, Shaoqing Ren, and Jian Sun. 2016. Deep residual learning for image recognition. In Proceedings of the IEEE conference on computer vision and pattern recognition. 770–778.
- [13] Yihui He, Xiangyu Zhang, and Jian Sun. 2017. Channel pruning for accelerating very deep neural networks. In Proceedings of the IEEE International Conference on Computer Vision. 1389–1397.
- [14] Gao Huang, Shichen Liu, Laurens Van der Maaten, and Kilian Q Weinberger. 2018. Condensenet: An efficient densenet using learned group convolutions. In Proceedings of the IEEE Conference on Computer Vision and Pattern Recognition. 2752–2764
- [15] Gao Huang, Zhuang Liu, Laurens Van Der Maaten, and Kilian Q Weinberger. 2017. Densely connected convolutional networks. In Proceedings of the IEEE conference on computer vision and pattern recognition. 4700–4708.
- [16] Diederik P Kingma and Jimmy Ba. 2014. Adam: A method for stochastic optimization. arXiv preprint arXiv:1412.6980 (2014).
- [17] Alex Krizhevsky, Ilya Sutskever, and Geoffrey E Hinton. 2012. Imagenet classification with deep convolutional neural networks. In Advances in neural information processing systems. 1097–1105.
- [18] Vadim Lebedev and Victor Lempitsky. 2016. Fast convnets using group-wise brain damage. In Proceedings of the IEEE Conference on Computer Vision and Pattern Recognition. 2554–2564.
- [19] Hao Li, Asim Kadav, Igor Durdanovic, Hanan Samet, and Hans Peter Graf. 2016. Pruning filters for efficient convnets. arXiv preprint arXiv:1608.08710 (2016).
- [20] Hao Li, Zheng Xu, Gavin Taylor, Christoph Studer, and Tom Goldstein. 2018. Visualizing the loss landscape of neural nets. In Advances in Neural Information Processing Systems. 6391–6401.
- [21] Chenxi Liu, Barret Zoph, Maxim Neumann, Jonathon Shlens, Wei Hua, Li-Jia Li, Li Fei-Fei, Alan Yuille, Jonathan Huang, and Kevin Murphy. 2018. Progressive neural architecture search. In Proceedings of the European Conference on Computer Vision (ECCV). 19–34.
- [22] Hanxiao Liu, Karen Simonyan, Oriol Vinyals, Chrisantha Fernando, and Koray Kavukcuoglu. 2017. Hierarchical representations for efficient architecture search. arXiv preprint arXiv:1711.00436 (2017).

- [23] Hanxiao Liu, Karen Simonyan, and Yiming Yang. 2018. Darts: Differentiable architecture search. arXiv preprint arXiv:1806.09055 (2018).
- [24] Zhuang Liu, Jianguo Li, Zhiqiang Shen, Gao Huang, Shoumeng Yan, and Chang-shui Zhang. 2017. Learning efficient convolutional networks through network slimming. In Proceedings of the IEEE International Conference on Computer Vision. 2736–2744.
- [25] Jian-Hao Luo, Jianxin Wu, and Weiyao Lin. 2017. Thinet: A filter level pruning method for deep neural network compression. In Proceedings of the IEEE international conference on computer vision. 5058–5066.
- [26] Risto Miikkulainen, Jason Liang, Elliot Meyerson, Aditya Rawal, Daniel Fink, Olivier Francon, Bala Raju, Hormoz Shahrzad, Arshak Navruzyan, Nigel Duffy, et al. 2019. Evolving deep neural networks. In Artificial Intelligence in the Age of Neural Networks and Brain Computing. Elsevier, 293–312.
- [27] Jongsoo Park, Sheng Li, Wei Wen, Ping Tak Peter Tang, Hai Li, Yiran Chen, and Pradeep Dubey. 2017. Faster cnns with direct sparse convolutions and guided pruning. In *International Conference on Learning Representations (ICLR)*.
- [28] Hieu Pham, Melody Y Guan, Barret Zoph, Quoc V Le, and Jeff Dean. 2018. Efficient neural architecture search via parameter sharing. arXiv preprint arXiv:1802.03268 (2018).
- [29] George Philipp and Jaime G Carbonell. 2017. Nonparametric neural networks. arXiv preprint arXiv:1712.05440 (2017).
- [30] Esteban Real, Sherry Moore, Andrew Selle, Saurabh Saxena, Yutaka Leon Suematsu, Jie Tan, Quoc V Le, and Alexey Kurakin. 2017. Large-scale evolution of image classifiers. In Proceedings of the 34th International Conference on Machine Learning-Volume 70. JMLR. org, 2902–2911.
- [31] Shreyas Saxena and Jakob Verbeek. 2016. Convolutional neural fabrics. In Advances in Neural Information Processing Systems. 4053–4061.
- [32] Karen Simonyan and Andrew Zisserman. 2014. Very deep convolutional networks for large-scale image recognition. arXiv preprint arXiv:1409.1556 (2014).
- [33] Leslie N Smith, Emily M Hand, and Timothy Doster. 2016. Gradual dropin of layers to train very deep neural networks. In Proceedings of the IEEE Conference on Computer Vision and Pattern Recognition. 4763–4771.
- [34] Kenneth O Stanley and Risto Miikkulainen. 2002. Evolving neural networks through augmenting topologies. Evolutionary computation 10, 2 (2002), 99–127.
- [35] Christian Szegedy, Wei Liu, Yangqing Jia, Pierre Sermanet, Scott Reed, Dragomir Anguelov, Dumitru Erhan, Vincent Vanhoucke, and Andrew Rabinovich. 2015. Going deeper with convolutions. In Proceedings of the IEEE conference on computer vision and pattern recognition. 1–9.
- [36] Tao Wei, Changhu Wang, and Chang Wen Chen. 2017. Modularized morphing of neural networks. arXiv preprint arXiv:1701.03281 (2017).
- [37] Tao Wei, Changhu Wang, Yong Rui, and Chang Wen Chen. 2016. Network morphism. In *International Conference on Machine Learning*. 564–572.
- [38] Wei Wen, Yuxiong He, Samyam Rajbhandari, Minjia Zhang, Wenhan Wang, Fang Liu, Bin Hu, Yiran Chen, and Hai Li. 2018. Learning intrinsic sparse structures within long short-term memory. In International Conference on Learning Representations (ICLR).
- [39] Wei Wen, Chunpeng Wu, Yandan Wang, Yiran Chen, and Hai Li. 2016. Learning structured sparsity in deep neural networks. In Advances in neural information processing systems. 2074–2082.
- [40] Huanrui Yang, Wei Wen, and Hai Li. 2020. DeepHoyer: Learning Sparser Neural Network with Differentiable Scale-Invariant Sparsity Measures. In International Conference on Learning Representations (ICLR).
- [41] Jaehong Yoon, Eunho Yang, Jeongtae Lee, and Sung Ju Hwang. 2017. Lifelong learning with dynamically expandable networks. arXiv preprint arXiv:1708.01547 (2017).
- [42] Barret Zoph and Quoc V Le. 2016. Neural architecture search with reinforcement learning. arXiv preprint arXiv:1611.01578 (2016).
- [43] Barret Zoph, Vijay Vasudevan, Jonathon Shlens, and Quoc V Le. 2018. Learning transferable architectures for scalable image recognition. In Proceedings of the IEEE conference on computer vision and pattern recognition. 8697–8710.